

# A Modified Approach to the Rack Generation of Beveloid Gears

Berat Gürçan Şentürk<sup>1,\*</sup> – Mahmut Cüneyt Fetvacı<sup>2</sup>

<sup>1</sup>Dogus University, Turkey

<sup>2</sup>Istanbul University-Cerrahpasa, Turkey

*The purpose of this paper is to present an easier and more efficient method for the determination of the geometry of a bevelled gear tooth. Based on a method that provides an easier way for the rack generation of involute helical gears, the mathematical model of a beveloid gear is studied. The mathematical procedure for developing two-dimensional cross-sections has been extended to three-dimensional gear models. A computer programme is developed to obtain generating and generated surfaces. The proposed algorithm is compared with the previous studies for verification and validation. The results demonstrate that the coordinates obtained from the given method are nearly the same on the start and end points of the main gear parts, such as the involute and root fillets regions. Also, between the limits, the values can be considered acceptable. A coordinate deviation of the gear profile has been observed in the mathematical model, because of the profile shift. Modifications have been developed in the equations to eliminate these cases. The main advantage of the proposed method is to obtain mathematical models without carrying out some of the calculation steps used in previous studies. Eventually, this feature will provide an easier and faster method to develop computer-aided models of the beveloid gear types.*

**Keywords:** beveloid gears, mathematical modelling, rack-type cutters, parametric modelling, involute profile

## Highlights

- An extended mathematical model for involute gears generated by rack-type cutters.
- Implementation differences between the given method and the previous methods have been compared.
- Avoiding the deviation of the profile caused by the profile shift.
- Coordinates of the critical points on the roots are analysed.

## 0 INTRODUCTION

Gear wheels, which are widely used in power transmission, have a wide range of applications from watches to automobiles, from printers to helicopters. In applications requiring high reliability, high strength, and low weight, simulating the physical behaviour of gear wheels in operating conditions before manufacturing saves time and material in the product development stage.

Numerical tools, such as the finite element method, are widely used to calculate the bending strength, contact stress, and transmission error of gear wheels. An accurate representation of the gear tooth geometry is essential for a reliable numerical analysis.

Rack-type cutters are widely used in the mass production of involute gears. A rack cutter is composed of three generating sections: involute, tip fillet, and top-land. The corresponding generated surfaces of a gear are the involute flank, trochoidal root fillet, and root bottom-land [1] and [2]. The mathematical equations of a gear tooth profile can be obtained based on the profile of the generating cutter, the manufacturing process, and gear meshing theory [3].

There are many studies on the mathematical modelling of gear wheels manufactured by rack

cutters in the literature [3], [4] and [5]. To mention some other studies as rack cutter modelling examples, Yang et al. have proposed a mathematical model for helical gears with asymmetric teeth [6]. Element construction and dynamic analysis have been made by Huang et al. for involute spur and helical gears [7]. Figliolini and Rea proposed a general algorithm for the kinematic synthesis of spur and helical gears and analysed the effects of the design parameters on the undercutting [8].

An approach for a mathematical model and contact analysis of helical gears was developed by Zeyin et al. [9]. Another parameterized approach to establish a high precision three-dimension finite element model of involute helical gears is proposed by Liu et al. [10]. In that study, a refinement methodology of the elements has been developed to improve the mesh quality and accuracy. A new tooth surface modelling method for beveloid gears has been proposed, and influences of the design parameters on the contact behaviours of parallel beveloid gears have been studied by Sun et al. [11]. Şentürk and Fetvacı have developed a mathematical method to prevent undercutting on the beveloid gear models [12]. Mesh stiffness is also a frequently studied topic for computerized gear modeling. A potential energy-based method was proposed by Song et al. to calculate the

mesh stiffness for straight beveloid gears with parallel axes. The effects of parameters, such as the pressure angle, pitch cone angle, and profile shift coefficient on the mesh stiffness were investigated [13]. Another mesh stiffness model has been generated by Zhou et al., which considers the direction variation of the tooth friction and wear influence on single gear–rack tooth pair mesh stiffness [14].

In another significant study, a calculation method of tooth profile modification for tooth contact analysis technology is proposed by Wang et al. [15]. In all the studies mentioned, the rack cutter generating method has been used in the modelling of gear geometries.

Litvin's Vector Approach, which also takes into account functional or production-required modifications, is widely used in the mathematical modelling of gear wheels. This approach also can be extended to all gear wheel modifications such as concave, crowning [16], parabolic modifications [17] and [18], non-circular gears [19] and cylindrical gears [20]. The mathematical model of the concave beveloid gears given, and contact simulations have been performed in [21]. Concave beveloid gears are also modelled and analysed in [22], [23] and [24]. The research on gear tooth modifications continues, such as the research on the external non-involute gear profiles. A review is made on this topic by Okorn et al. [25]. Also, experimental research investigates the characteristics and increases the performance of the gear systems, such as the electrical control anti backlash method proposed by Wang et al. [26] and the experimental study and numerical analysis on aviation spiral bevel gear made by Li et al. [27].

By generalizing the mathematical model for parallel axis gears, a model including spur, helical, straight beveloid, and helical beveloid gears can be obtained [4], [5] and [7]. A beveloid gear can be generated by a basic rack whose pitch plane intersects with the axis of the gear and forms an angle equal to the generating cone angle [4].

In the computer simulation of gear wheels, the vector representation of the generating tool is first established. Usually, equations are expressed in the normal section. Coordinate transformation is performed in the case of helical and/or conical geometries. Then, the cutter geometry at the transverse section is expressed in the coordinate system of the gear to be manufactured. The next step is to establish the equation of meshing by using differential geometry and gear theory. Thus, the mathematical model of the gear wheel is obtained.

In the publications mentioned above, the coordinate systems used for determining the tool geometries may be oriented differently. The right-hand type of a cartesian coordinate system is preferred. Analytical description of the rack tooth geometry and intervals of curvilinear parameters may change due to the orientation of the coordinate system attached to the generating cutter. In most of the papers engineering approach to differential geometry proposed by Litvin is used to establish the equation of meshing. In Batista's study [28], the origin of the coordinate system, unlike with other researchers, is located at the point where the pitch line intersects the involute edge, as illustrated in Fig. 1 compared to other studies, Batista did not use the directional cosines of the cutter surface vector in the determination of the equation of meshing. The steps followed in modelling provide ease of computer programming.

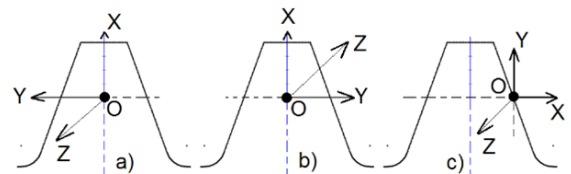


Fig. 1. Different coordinate systems for normal section of rack cutter

The mathematical models of beveloid gears generated by rack-type cutters are studied in various research works [7], [11] and [12]. The aim of this study is to extend the mathematical model proposed by Batista to beveloid (involute conical) gearing. This way, when compared to the previous studies, the gear tooth geometry can be expressed in a much simpler form, depending on the roll angle. Also, the gear simulation process will be less time consuming by shortening the modelling algorithm.

In scope of this work, the design steps of the proposed modelling method are given clearly, by showing the mathematical equations of the design parameters, including the modifications for the conical and beveloid gear geometries. Gear tooth profiles drawn by the previous studies and the present method are compared, and finally, the modelling algorithms are shown.

## 1 METHODS

According to one of the previous methods proposed by Liu et al. [4], a beveloid gear can be modelled by defining the rack cutter geometry and simulating the translation and rotation of the cutter around the global

$$y_L = \begin{cases} u & -\frac{m_n \pi}{4} \leq x_L \leq -u \tan(\alpha_{n1,2}) \\ -\frac{x_L}{\tan(\alpha_{n1,2})} & -u \tan(\alpha_{n1,2}) \leq x_L \leq m_n \tan(\alpha_{n1,2}) \\ y_{L0} - \sqrt{(\rho_{1,2})^2 - (x_{L0} - x_L)^2} & m_n \tan(\alpha_{n1,2}) \leq x_L \leq x_{L0} \\ -m_n - c_n & x_{L0} \leq x_L \leq \frac{m_n \pi}{4} \end{cases}, \quad (1)$$

coordinate system origin,  $S_C$ . Dimensions of the rack cutter design parameters are given in Fig. 2. Also, the figure shows the asymmetrical state, in which both tapered and helical hobbing conditions exist in the gear model.

$$\begin{aligned} \rho_{1,2} &= \frac{c_n}{1 - \sin(\alpha_{n1,2})}, \\ x_{L0} &= m_n \tan(\alpha_{n1,2}) + \rho_{1,2} \cos(\alpha_{n1,2}), \\ y_{L0} &= -m_n + \rho_{1,2} \sin(\alpha_{n1,2}). \end{aligned} \quad (2)$$

For plotting, we can define the tool geometry in the global cartesian coordinate system  $S_0$ , as written in Eq. (3).

$$\begin{bmatrix} x_N \\ y_N \end{bmatrix} = \begin{bmatrix} x_L \\ y_L \end{bmatrix} + \begin{bmatrix} \mp 0.25 m_n \pi \\ 0 \end{bmatrix}. \quad (3)$$

On Eq. (3), the + and - signs are for the left and right side of the rack, respectively.

Eq. (3) draws only one of the rack cutter profiles for the zero position in 2D. The rack cutter cross-section is translated by  $r_i \varphi$  and rolled by an angle which is one of the major design parameters  $\varphi$ . After the translation and rotation processes, two-dimensional cross-section of the beveloid gear, which has an asymmetrical profile due to the helix and cone angles, is drawn by the imaginary motion of the inclined rack cutter cross-sections (see Fig. 3).

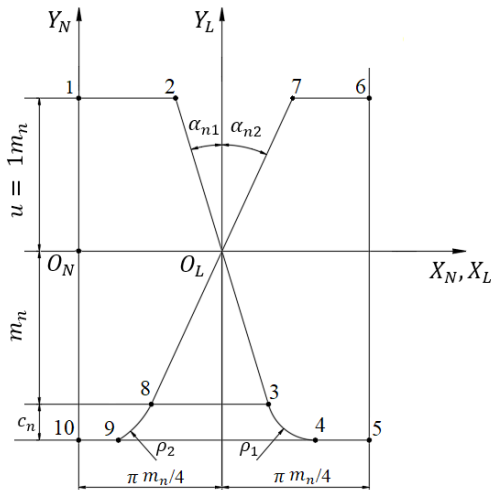


Fig. 2. The configuration of rack cutter and reference coordinate system

In Eq. (1), the equations that define the beveloid tooth profile can be simplified according to the position of this chosen coordinate system. Because of this orientation, intervals of the design parameters can be changed when compared to previous studies [4], [6], [12].

Fig. 2 shows that the rack cutter coordinate system is placed over the involute section. The angles  $\beta$  and  $\delta$  are the helical and cone angles of the gear tooth, respectively.

From Fig. 2, the coordinates can be defined analytically by Eq. (1).

Here, the radius of the root fillets  $\rho_1$  and  $\rho_2$  and the origin coordinates  $x_{L0}$  and  $y_{L0}$  of the rack coordinate system  $S_L$  can be expressed as:

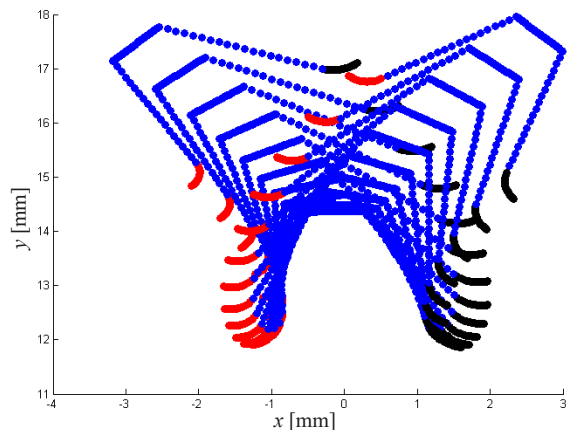


Fig. 3. The rack cutter generation process for beveloid gears

Because of the helix and cone angles, the position of the rack cutter should be turned around the horizontal and vertical axis  $X_N$  and  $Y_N$ , by the amount of  $\delta$  and  $\beta$ , respectively. The rotation matrices are given in Eq. (4).

$$\mathbf{M}_{CP} = \begin{bmatrix} 1 & 0 & 0 & 0 \\ 0 & \cos(\delta) & -\sin(\delta) & 0 \\ 0 & \sin(\delta) & \cos(\delta) & 0 \\ 0 & 0 & 0 & 1 \end{bmatrix},$$

$$\mathbf{M}_{PN} = \begin{bmatrix} \cos(\beta) & 0 & -\sin(\beta) & \lambda \sin(\beta) \\ 0 & 1 & 0 & 0 \\ \sin(\beta) & 0 & \cos(\beta) & -\lambda \cos(\beta) \\ 0 & 0 & 0 & 1 \end{bmatrix}. \quad (4)$$

$$\mathbf{R}_C = \begin{bmatrix} x_C \\ y_C \\ z_C \end{bmatrix} = \begin{bmatrix} x_N \cos(\beta) - \lambda \sin(\beta) \\ -x_N \sin(\delta) \sin(\beta) + y_N \cos(\delta) - \lambda \sin(\delta) \cos(\beta) \\ -y_N \sin(\delta) - x_N \cos(\delta) \sin(\beta) + \lambda \cos(\delta) \cos(\beta) \end{bmatrix}. \quad (5)$$

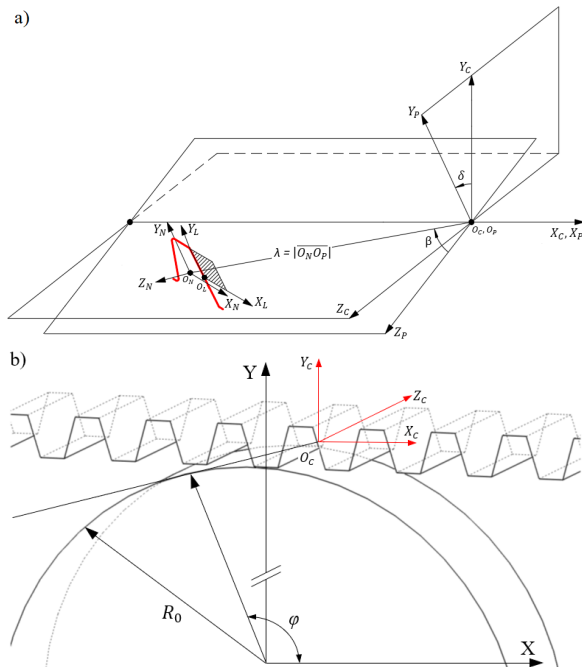


Fig. 4. Relations among the coordinate systems

By applying these coordinate transformations, we can obtain tooth geometry in the  $S_C$  coordinate system.

The term  $\lambda$  states the translation of the origin  $O_C$  and is integrated into the matrix  $\mathbf{M}_{PN}$ .

If the third row of Eq. (5) is rearranged for  $z_C = z$ , the parameter  $\lambda$  can be calculated as in Eq. (6). With the help of this parameter, a two-dimensional cross-section of the rack can be defined.

$$\lambda = \frac{z + y_N \sin(\delta) + x_N \cos(\delta) \sin(\beta)}{\cos(\beta) \cos(\delta)}. \quad (6)$$

On the analytical definitions, different from the formulations given in the previous studies, normal vectors are not used. Instead, the meshing condition is simulated with the help of partial derivatives. Finally, the parametric equations for the geometric positions of the rack cutter have been derived.

As explained earlier, the global and rack coordinate systems are defined and can be seen in Fig. 4. The relation between these systems can be expressed as:

$$X = X_0 + x_N \sin(\varphi) + y_N \cos(\varphi), \quad (7)$$

$$Y = Y_0 - x_N \cos(\varphi) + y_N \sin(\varphi). \quad (8)$$

The involute of the circle, which described by the origin of the rack coordinate system  $S_0$ , can be defined as:

$$X_0 = R_0 \cos(\varphi) + R_0 \varphi \sin(\varphi), \quad (9)$$

$$Y_0 = R_0 \sin(\varphi) - R_0 \varphi \cos(\varphi). \quad (10)$$

The vertical position of the rack cutter should be redefined due to the profile shift  $e$ . The equation of the generated gear tooth surface at the transverse section can be explained by Eq. (12).

$$y_N \rightarrow y_N + e, \quad (11)$$

$$X = (R_0 + e + y_C) \cos(\varphi) + (R_0 \varphi + x_C) \sin(\varphi), \quad (12)$$

$$Y = (R_0 + e + y_C) \sin(\varphi) - (R_0 \varphi + x_C) \cos(\varphi). \quad (13)$$

In Eqs. (11) to (13), parameters  $x_C$  and  $y_C$  can be defined as  $x_C = x_C(s)$  and  $y_C = y_C(s)$ . Here  $s$  is defined as an arbitrary continuous parameter.

To be able to calculate the roll angle  $\varphi$ , the condition during the meshing of the gears in contact can be written as in Eq. (14),

$$\frac{\delta X}{\delta \varphi} \frac{\delta Y}{\delta s} - \frac{\delta Y}{\delta \varphi} \frac{\delta X}{\delta s} = 0. \quad (14)$$

After the parameters in Eqs. (12) and (13) are differentiated, and plugged, in Eq. (14) the roll angle  $\varphi$  can be calculated as,

$$\varphi(x_c) = -\frac{1}{R_0} [x_c + e + y_c] \frac{dy_c}{dx_L} \quad (15)$$

Here, the value for the derivative  $\frac{dy_c}{dx_L}$  can be written as in Eq. (16):

$$\frac{dy_c}{dx_L} = \begin{cases} 0 \\ \pm \frac{1}{\tan(\alpha_{r1,2})} \\ \frac{x_{L0} - x_L}{\sqrt{(\rho_{1,2})^2 - (x_{L0} - x_L)^2}} \tan(\alpha_{n1,2}) \\ 0 \end{cases}, \quad (16)$$

By using Eqs. (5), (6), (12), (13), (15) and (16), we can obtain generated gear geometry in the plane of rotation (in transverse section).

In this manner, a three-dimensional beveloid gear tooth can be modelled with the help of changed cross-sections with respect to coordinate  $z$ .

In Eq. (16),  $\alpha_{r1,2}$  is included in the formulation to state the pressure angle on the transverse plane. If not, because of the helical and conical properties, this condition will cause geometric irregularities on the involute section and the root fillets. This modification is one of the major changes made in the mathematical models proposed by Batista [28].

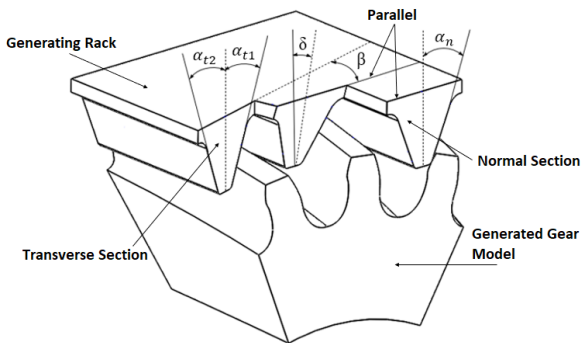


Fig. 5. Generating rack and generated gear in mesh

$$\alpha_{r1} = (\tan)^{-1} \left( \frac{\cos(\delta) \sin(\alpha_{n1}) - \cos(\alpha_{n1}) \sin(\beta) \sin(\delta)}{\cos(\alpha_{n1}) \cos(\beta)} \right), \quad (17)$$

$$\alpha_{r2} = (\tan)^{-1} \left( \frac{\cos(\delta) \sin(\alpha_{n2}) + \cos(\alpha_{n2}) \sin(\beta) \sin(\delta)}{\cos(\alpha_{n2}) \cos(\beta)} \right). \quad (18)$$

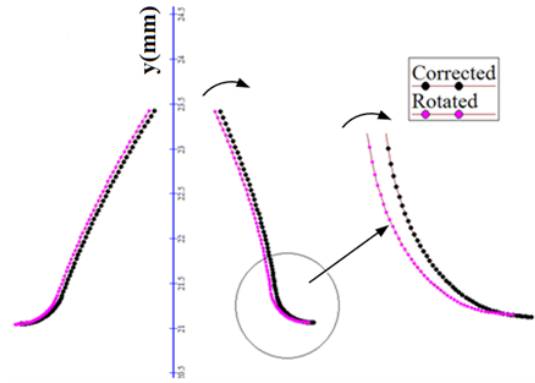


Fig. 6. Generating rack and generated gear in mesh

This relationship can be seen in Fig. 5. The equations of “ $\alpha_{r1,2}$ ” on each side of the rack can be written as in Eqs. (17) and (18). These expressions are proposed on the previous works by Liu and Tsay [4].

It has been observed in the present mathematical model that the conventional profile shift causes coordinate deviation of the generated helical beveloid gear. To compensate for this deviation, gear blank is re-rotated by the angle  $\gamma$ .

$$e = \frac{e_n}{\cos(\delta)}, \quad (19)$$

$$\gamma = e \tan(\beta) \frac{\sin(\delta)}{R_0} \text{ or } \gamma = e_n \tan(\beta) \frac{\tan(\delta)}{R}. \quad (20)$$

Fig. 6 shows this effect for the parameters,  $m_n = 1 \text{ mm}$ ,  $z = 40$ ,  $\delta = 14^\circ$ ,  $\beta = 24^\circ$ ,  $e_n = 0.5 m_n$ . For this case, the deflection is  $2.53527\text{e-}03 \text{ rad}$  ( $0.1452603^\circ$ ).

$$R_0 = \frac{m_n z}{2} \cos(\beta). \quad (21)$$

After defining the deflection angle, the correction can be made by following

$$\mathbf{R}_G = \begin{bmatrix} X_G \\ Y_G \\ Z_G \end{bmatrix} = \begin{bmatrix} \cos(\gamma) & \sin(\gamma) & 0 \\ -\sin(\gamma) & \cos(\gamma) & 0 \\ 0 & 0 & 1 \end{bmatrix} \begin{bmatrix} X_c \\ Y_c \\ Z_c \end{bmatrix}. \quad (22)$$

After multiplying the gear profile coordinates by the correction matrix in Eq. (22), gear coordinates with the profile shift,  $X_G$ ,  $Y_G$  and  $Z_G$  can be obtained.

### 1.1 Gear Generation

After generating the tooth profiles in two dimensions, cross-section geometries can be combined using

geometric methods offered by computer-aided design (CAD) software. After modelling the single gear tooth, the 3D geometries can be duplicated.

Fig. 7a displays the change in geometry through the tooth width. By using these cross-section geometries, solid models of beveloid gears can be built. Consecutive cross-sections form the tooth surfaces as seen in Figs. 7b and in c the complete model is seen.

Fig. 8a displays the geometric parameters of the designed beveloid gear pair, such as the centre distance, tip and root diameters and the tooth thickness. The design parameters are:  $m_n = 3$  mm,

$z = 24$ ,  $\alpha_{n1} = \alpha_{n2} = 20^\circ$ ,  $\delta = 15^\circ$ ,  $\beta = 15^\circ$  for both pinion and gear.

The 3D models of the gear geometries has been produced by 3D printer using, fused deposition modelling (FDM) technique. It can be seen on Figs. 8b and c that the tooth thickness is becoming smaller, and undercutting can start to occur on the side where the height of the root region is the greatest and becoming larger on the other side where the root height is the smallest. Gear geometries in both Figs. 8b and c are the same, but the gears are flipped.

Fig. 9 displays the generation algorithms of previous studies in Fig. 9a and the proposed method

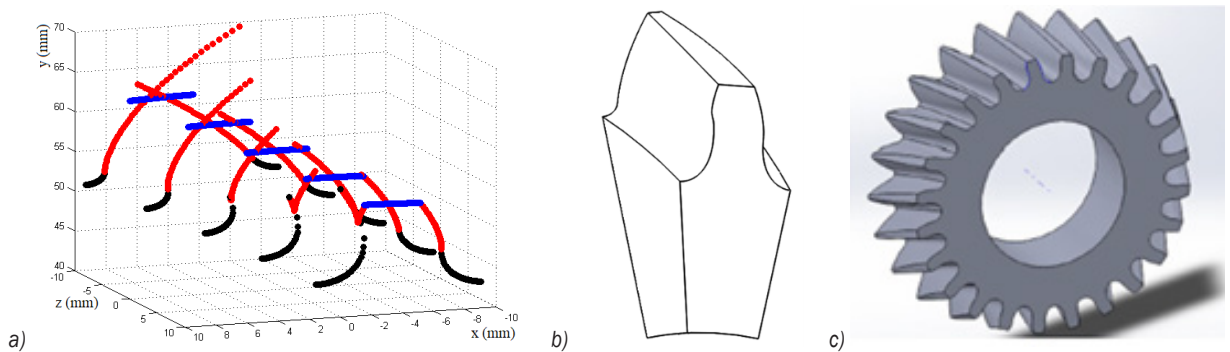


Fig. 7. Beveloid gear generation steps

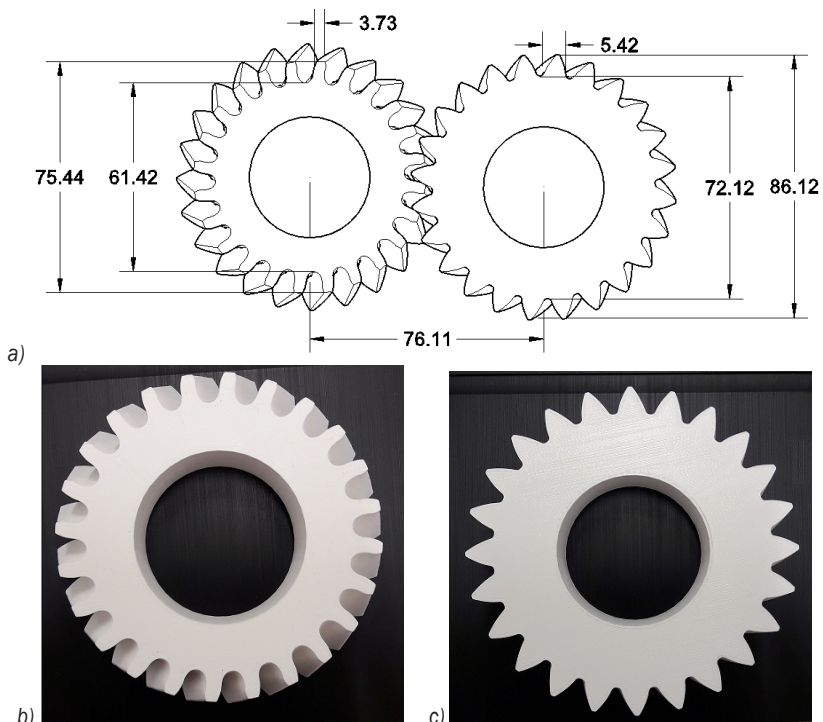


Fig. 8. Geometric parameters of the gear pair and generated beveloid gears;

a) beveloid gear pair on parallel axes, b) and c) views form the front and back sides of the beveloid gear model respectively

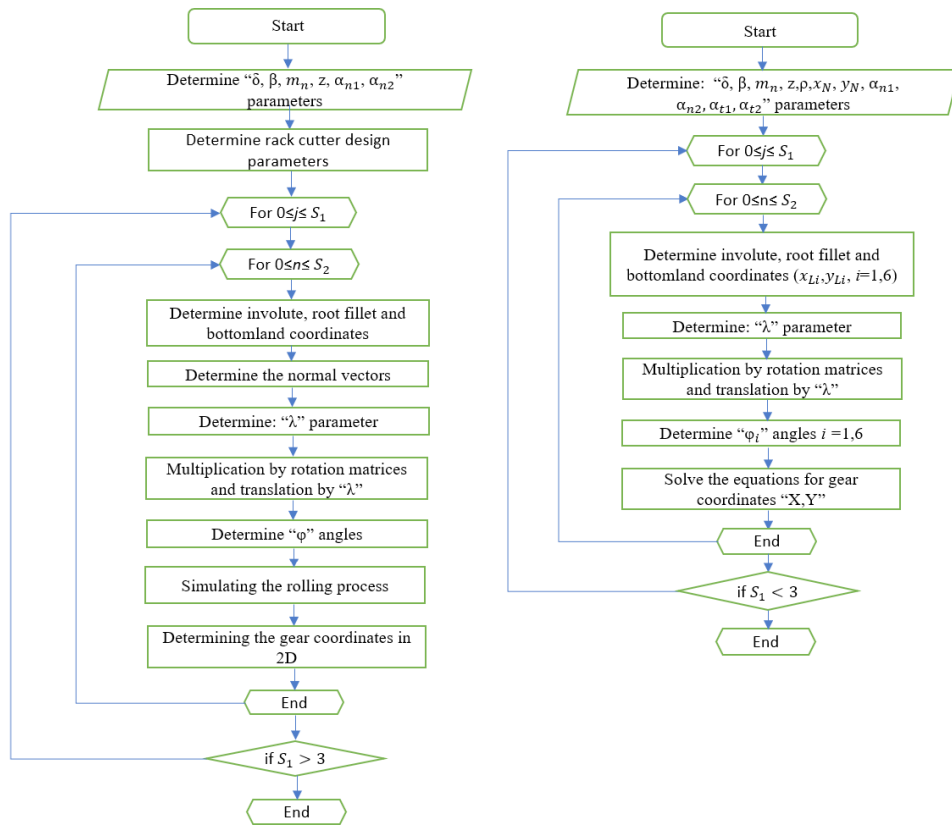


Fig. 9. Gear generation algorithms a) previous studies, b) proposed method

in Fig. 9b. It has seen that the calculating algorithm is shortened. For this reason, the modelling process for the proposed model becomes much simpler and less time consuming. For the cross-section generation, values for the roll angle “ $\varphi_i$ ” is calculated by meshing equation Eq. (15). In this manner, the definition of normal vectors will not be necessary. As seen in Eq. (A8) the normal vector equation is a function of both the “ $l_R$ ” and “ $\lambda$ ” parameters. The symbolic definition of a normal vector becomes large and hard to calculate after the cross multiplication operations. With the help of the new proposed method, gear cross-sections can be drawn directly from coordinate definitions “ $X$  and  $Y$ ” as in Eqs. (5) and (6).

## 2 RESULTS

Based on the proposed mathematical model, a program is developed to obtain generating and generated surfaces.

Fig. 10 displays cross-section geometries of beveloid gears for design parameters ...  $m_n = 4$  mm,  $z$

$= 25$ ,  $\alpha_{n1} = \alpha_{n2} = 20^\circ$ ,  $\delta = 20^\circ$ ,  $\beta = 0^\circ$  for Fig. 10a and  $\delta = 20^\circ$ ,  $\beta = 20^\circ$  for Fig. 10b.

The same parameters are also used in Figs. 11 to 13.

Fig. 11 shows the comparison of the gear tooth geometries drawn by the previous and the new proposed method. It is clearly seen that the position coordinates are nearly the same. Here, the helical and cone angles are the same as in Fig. 10b.

After the mathematical model for the two-dimensional cross-sections has been completed, the involute and root fillet regions are compared with the previous models. Figs. 11 and 12 show the change in the root fillets due to tooth width and cone angle  $\delta$  respectively.

As seen in Fig. 12, the distance between the position coordinates of the root fillet regions is sensitive to the excessive undercut cases. These situations can occur either with the increase in the cone angle or the change in the tooth width through undercut sections. Mathematically, this inconsistency is caused by the square root terms in the root fillet definitions of the proposed model.

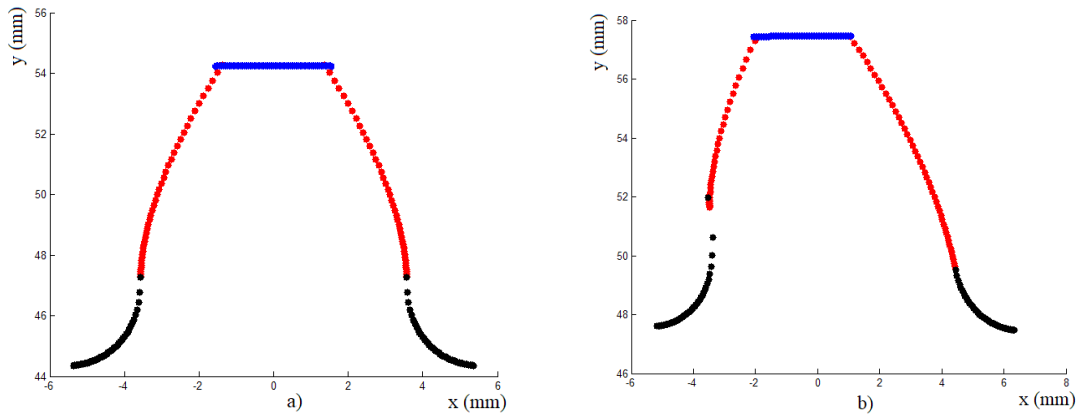


Fig. 10. 2D cross-sections of conical and beveloid gear models; a) non-helical, b) helical beveloid gear models

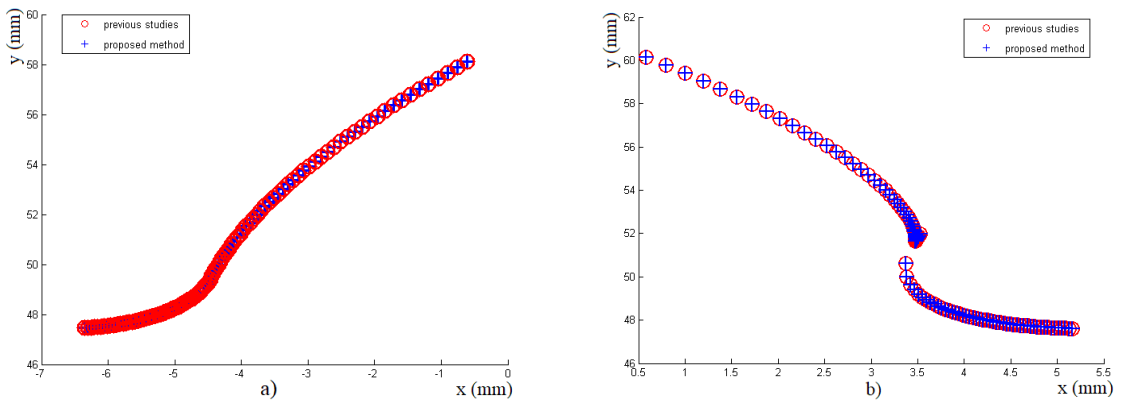


Fig. 11. Comparison of conventional method and the method proposed by Batista [28] in 2D; a) the side with no undercut, and b) undercut side

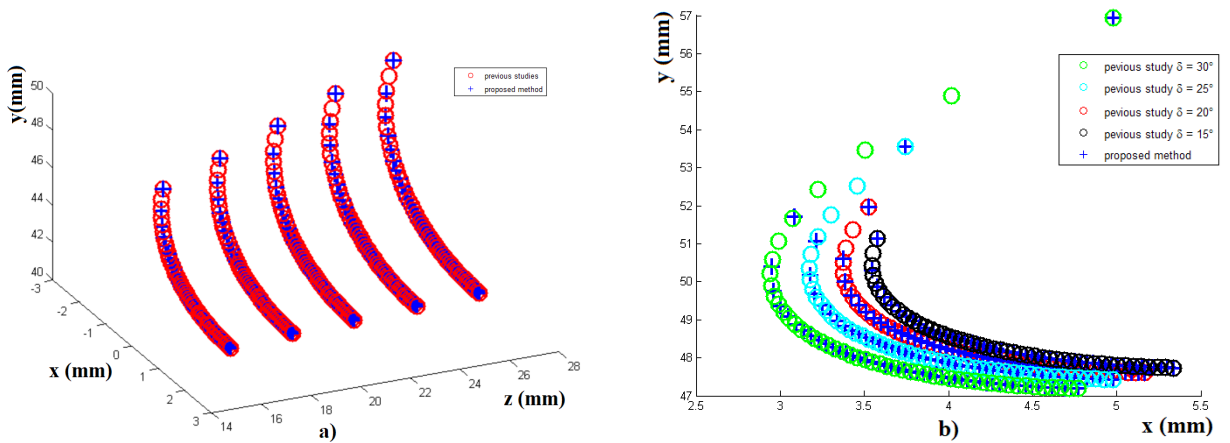
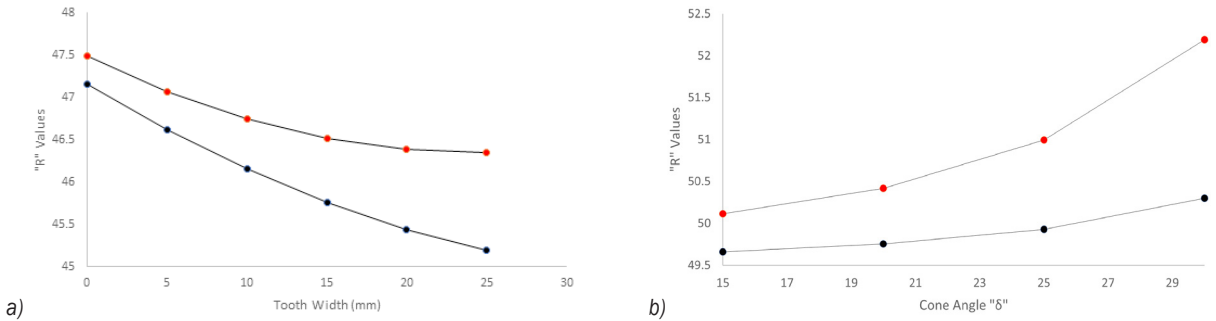


Fig. 12. The root fillet coordinates of 2D beveloid gear models generated by previous and new developed methods; a)  $\delta = 10^\circ$ ,  $\beta = 10^\circ$  and  $z = 15$  mm to 25 mm, and b)  $\delta = 15^\circ$  to  $30^\circ$ ,  $\beta = 20^\circ$

Fig. 13 indicates the same result, by comparing the radius values  $R$ , which is the square root of sum of square values of horizontal and vertical position coordinates. The coordinate values are chosen from

the regions where the root fillets are connected to the involute sections.

At high cone angle values, undercutting starts to occur. The patterns do not follow the geometric



**Fig. 13.** The change in radius values  $R$  based on the change in a) tooth width, and b) cone angle  $\delta$

contour around the undercut regions of the models drawn by previous methods. Nevertheless, the two-dimensional geometries are compatible with the previous ones on the end points of the root fillets. In general applications, cone angles are not selected as high values to cause undercutting problems (mostly up to  $15^\circ$ ). Because of that, deviation cases do not cause serious modelling errors.

Consequently, the variation between the calculation algorithms cause a relatively small difference in the coordinates when undercutting status is concerned. This condition can be fixed by practical geometric techniques offered by CAD programs. Also, the results shows that the differences between the coordinate values are within acceptable limits.

### 3 CONCLUSION

In this study, Batista's mathematical model for rack generation [28] has been extended to beveloid gears. That model was developed for 2D cross-sections; the modified equations in the proposed method allows for model gear geometries in three dimensions by changing the cross-section accurately, considering the effect of the cone angle.

The mathematical equations are given briefly, and the modelling algorithms are compared with the previous method proposed by Liu and Tsay [4]. It has been seen that the gear tooth profiles generated by the two methods overlap very closely with each other.

Also, while adapting of the equations, it has been observed that the profile shift parameters cause the cross-sections to rotate by a small angle around the tooth width axis for beveloid geometries. To avoid that, a modification angle has been developed and included in the equations.

The detailed investigation on the root fillet regions for helical and conical cases showed that the change in the position coordinates is within acceptable limits.

It is obvious that the modelling technique proposed by Batista [28] makes it easier to define the gear cross-section geometries and enables the designers to avoid time-consuming techniques.

In this way, especially for the computer simulations of gears, modelling the point clouds and tooth surfaces of the involute, root fillet, bottom land, and tip regions of the beveloid gears will be easier and less time-consuming.

The mathematical model proposed in this study, can be extended to different gear geometries such as non-circular, cylindrical gears, and curvilinear gear teeth [19], [20] and [29], and internal gears [30]. Also parabolic modification [17] and [18] and generating cutter can be considered [31] to [33].

### 4 NOMENCLATURES

$\delta$	cone angle, $[\circ]$
$\beta$	helix angle, $[\circ]$
$\rho_{1,2}$	root fillet radius, [mm]
$c_n$	clearance, [mm]
$u$	addendum, [mm]
$m_n$	normal module, [mm]
$\alpha_{n1,2}$	pressure angle on normal plane, $[\circ]$
$\alpha_{t1,2}$	pressure angle on transverse plane, $[\circ]$
$z$	gear tooth width, [mm]
$\varphi$	roll angle, $[\circ]$
$e$	profile shift in transverse section, [mm]
$e_n$	profile shift in normal section, [mm]
$\gamma$	deflection angle, $[\circ]$
$R_0$	pitch circle radius, [mm]

### 5 REFERENCES

- [1] Jelaska, D. (2012). Gears and Gear Drives. John Wiley & Sons, Chichester, DOI:10.1002/9781118392393.
- [2] Vullo, V. (2020). Gears. Spinger, Cham, DOI:10.1007/978-3-030-40164-1.

- [3] Litvin, F.L., Fuentes, A. (2004). *Gear Geometry and Applied Theory*. Cambridge University Press, Cambridge, DOI:10.1017/CB09780511547126.
- [4] Liu, C.-C., Tsay, C.-B. (2001). Tooth undercutting of beveloid gears. *Journal of Mechanical Design*, vol. 123, no. 4, p. 569-576, DOI:10.1115/1.1414128.
- [5] Brauer, J. (2004). A general finite element model of involute gears. *Finite Elements in Analysis and Design*, vol. 40, no. 13-14, p. 1857-1872, DOI:10.1016/j.finel.2004.02.002.
- [6] Yang, S.-C.. (2005). Mathematical model of a helical gear with asymmetric involute teeth and its analysis. *The International Journal of Advanced Manufacturing Technology*, vol. 26, p. 448-456, DOI:10.1007/s00170-003-2033-z.
- [7] Huang, K.J., Wei Su, H.. (2010). Approaches to parametric element constructions and dynamic analyses of spur/helical gears including modifications and undercutting. *Finite Elements in Analysis and Design*, vol. 46, no. 12, p. 1106-1113, DOI:10.1016/j.finel.2010.08.002.
- [8] Figliolini, G., Rea, P. (2014). Effects of the design parameters of involute gears generated by rack-cutters. *International Gear Conference*, p. 294-302, DOI:10.1533/9781782421955.294.
- [9] He, Z., Lin, T., Luo, T., Deng, T., Hu, Q. (2016). Parametric modeling and contact analysis of helical gears with modifications. *Journal of Mechanical Science and Technology*, vol. 30, p. 4859-4867, DOI:10.1007/s12206-016-1004-x.
- [10] Liu, Y., Zhao, Y., Liu, M., Sun, X. (2019). Parameterized high-precision finite element modelling method of 3D helical gears with contact zone refinement. *Shock and Vibration*, vol. 2019, art ID 5809164, DOI:10.1155/2019/5809164.
- [11] Sun, R., Song, C., Zhu, C., Liu, S., Wei, C. (2020). Tooth surface modelling and mesh behaviors for paralleled beveloid gears. *Journal of Mechanical Design*, vol. 142, no. 5, art. ID 054501, DOI:10.1115/1.4045141.
- [12] Şentürk, B.G., Fetvacı, M.C. (2020). Modelling and undercutting analysis of beveloid gears. *Journal of the Faculty of Engineering and Architecture of Gazi University*, vol. 35, no. 2, p. 901-916, DOI:10.17341/gazimmfd.544038. (in Turkish)
- [13] Song, C., Zhou, S., Zhu, C., Yang, X., Li, Z., Sun, R. (2018). Modeling and analysis of mesh stiffness for straight beveloid gear with parallel axes based on potential energy method. *Journal of Advanced Mechanical Design, Systems, and Manufacturing*, vol. 12, no. 7, (2018): art. ID JAMDSM0122, DOI:10.1299/jamdsm.2018jamdsm0122.
- [14] Zhou, C., Dong, X., Wang, H., Liu, Z. (2022). Time-varying mesh stiffness model of a modified gear-rack drive with tooth friction and wear. *Journal of the Brazilian Society of Mechanical Sciences and Engineering*, vol. 44art. ID 213, DOI:10.1007/s40430-022-03517-8.
- [15] Wang, C. Wang, S., Wang, G. (2018). A calculation method of tooth profile modification for tooth contact analysis technology. *Journal of the Brazilian Society of Mechanical Sciences and Engineering*, vol. 40 art. ID 341, DOI:10.1007/s40430-018-1268-4.
- [16] Wang, H., Zhou, C., Hu, B., Liu, Z. (2019). Tooth wear prediction of crowned helical gears in point contact. *Proceedings of the Institution of Mechanical Engineers, Part J: Journal of Engineering Tribology*, vol. 234, no. 6, p. 947-963, DOI:10.1177/1350650119896467.
- [17] Chen, Y.-J., Yang, H.-C., Pai, P.F. (2016). Design and kinematics evaluation of a gear pair with asymmetric parabolic teeth. *Mechanism and Machine Theory*, vol. 101, p. 140-157, DOI: 10.1016/j.mechmachtheory.2016.03.008.
- [18] Ni, G., Zhu, C., Song, C., Du, X., Zhou, Y. (2017). Tooth contact analysis of crossed beveloid gear transmission with parabolic modification. *Mechanism and Machine Theory*, vol. 113, p. 40-52, DOI:10.1016/j.mechmachtheory.2017.03.004.
- [19] Wu, L., Han, J., Zhu, Y., Tian, X., Xia, L.. (2017). Non-circular gear continuous generating machining interpolation method and experimental research. *Journal of the Brazilian Society of Mechanical Sciences and Engineering*, vol. 39, p. 5171-5180, DOI:10.1007/s40430-017-0873-y.
- [20] Jia, K., Guo, J., Zheng, S., Hong, J. (2019). A general mathematical model for two-parameter generating machining of involute cylindrical gears. *Applied Mathematical Modelling*, vol. 75, p. 37-51, DOI:10.1016/j.apm.2019.05.021.
- [21] Liu, C.-C., Tsay, C.-B. (2002). Mathematical models and contact simulations of concave beveloid gears. *Journal of Mechanical Design*, vol. 124, no. 4, p. 753-760, DOI:10.1115/1.1517563.
- [22] Liu, S., Song, C., Zhu, C., Fan, Q. (2018). Concave modifications of tooth surfaces of beveloid gears with crossed axes. *Proceedings of the Institution of Mechanical Engineers, Part C: Journal of Mechanical Engineering Science*, vol. 233, no. 4, p. 1411-1425, DOI:10.1177/0954406218768842.
- [23] Liu, C.-C., Chen, Y.-C., Lin, S.-H. (2010). Contact stress analysis of straight concave conical involute gear pairs with small intersected angles. *Proceedings of the International MultiConference of Engineers and Computer Scientists*, vol. 3.
- [24] Liu, C.-C., Chen, Y.-C., Peng, Y.-L. (2015). Contact pattern simulation and stress analysis of intersected concave conical involute gear pairs generated by shaper cutters. *Proceedings of the 14th IFToMM World Congress*, DOI:10.6567/IFTToMM.14TH.WC.PS6.007.
- [25] Okorn, I., Nagode, M., Klemenc, J. (2021). Operating performance of external non-involute spur and helical gears: A Review. *Journal of Mechanical Engineering - Strojnikski vestnik*, vol. 67, no. 5, p. 256-271, DOI:10.5545/sv-jme.2020.7094.
- [26] Wang, G., Zhu, D., Zou, S., Jiang, Y., Tian, X. (2022). Simulation and experimental research on electrical control anti-backlash based on a novel type of variable tooth thickness involute gear pair. *Strojnikski vestnik - Journal of Mechanical Engineering*, vol. 68, no. 2, p. 126-140, DOI:10.5545/sv-jme.2021.7452.
- [27] Li, L., Wang, S. (2023). Experimental study and numerical analysis on windage power loss characteristics of aviation spiral bevel gear with oil injection lubrication. *Strojnikski vestnik - Journal of Mechanical Engineering*, vol. 69, no. 5-6, p. 235-247, DOI:10.5545/sv-jme.2023.558.
- [28] Batista, M. (2021). Analytical treatment of the geometry of involute gears. *ResearchGate*, DOI:10.13140/RG.2.2.31057.66404.
- [29] Tseng, R.-T., Tsay, C.-B. (2004). Contact characteristics of cylindrical gears with curvilinear shaped teeth. *Mechanism and Machine Theory*, vol. 39, no. 9, p. 905-919, DOI:10.1016/j.mechmachtheory.2004.04.006.
- [30] Yan, G., Song, C., Zhu, F., Cui, Z., Deng, Z. (2022). The analysis of contact ratio of involute internal beveloid gears with small tooth difference. *Journal of Advanced Mechanical*

*Design, Systems, and Manufacturing*, vol. 16, no. 1, art. IDJAMDSM0017, DOI:10.1299/jamdsm.2022jamdsm0017.

- [31] Lai, C.-H., Yang, H.-C. (2016). Theoretical investigation of a planar rack cutter with variable diametral pitch. *Arabian Journal for Science and Engineering*, vol. 41, p. 1585-1594, DOI:10.1007/s13369-015-1856-x.
- [32] Yang, S.-C. (2006). A study on using deviation function method to reshape a rack cutter. *The International Journal of Advanced Manufacturing Technology*, vol. 30, p. 385-394, DOI:10.1007/s00170-005-0089-7.
- [33] Cao, B., Li, G. (2021). Computerized design of plunge shaving tool for beveloid gears and plunge shaving characteristic analysis. *Mechanism and Machine Theory*, vol. 161, art. ID 104325, DOI:10.1016/j.mechmachtheory.2021.104325.

## 6 APPENDIX

### Comparison of Mathematical Models

The calculation process due to the generation method proposed by Liu and Tsay [4] is explained in detail.

The coordinates of the involute section is:

$$\mathbf{R}_n^R = \begin{bmatrix} x_n^R \\ y_n^R \\ z_n^R \end{bmatrix} = \begin{bmatrix} b_c - l_R \sin(\alpha_{n1}) + c_y \pi m_n \\ l_R \cos(\alpha_{n1}) \\ 0 \end{bmatrix}. \quad (A1)$$

Here  $l_R$  is the coordinates of the involute section of the rack, where:

$$\frac{-a_c}{\cos(\alpha_{n1})} \leq l_R \leq \frac{a_t}{\cos(\alpha_{n1})}, \quad (A2)$$

where  $a_c$  and  $a_t$  are addendum and dedendum values respectively and equal to normal module  $m_n$  and  $b_c = 0.25 \pi m_n$ .

The value  $c_y$  can be determined as 0, 1, 2, ... so that the rack cutter and generated gear can be modeled with desired number of teeth.

The rotation matrices for the cone and helix angles can be written as:

$$\mathbf{M}_{cp} = \begin{bmatrix} 1 & 0 & 0 & 0 \\ 0 & \cos(\delta) & -\sin(\delta) & 0 \\ 0 & \sin(\delta) & \cos(\delta) & 0 \\ 0 & 0 & 0 & 1 \end{bmatrix}, \quad (A3)$$

$$\mathbf{M}_{pn} = \begin{bmatrix} \cos(\beta) & 0 & -\sin(\beta) & \lambda \sin(\beta) \\ 0 & 1 & 0 & 0 \\ \sin(\beta) & 0 & \cos(\beta) & -\lambda \cos(\beta) \\ 0 & 0 & 0 & 1 \end{bmatrix}. \quad (A4)$$

By multiplying  $\mathbf{M}_{cp}$  with  $\mathbf{M}_{pn}$ ,  $\mathbf{M}_{cn}$  can be written as:

$$\mathbf{M}_{cn} = \begin{bmatrix} \cos(\beta) & 0 & -\sin(\beta) & \lambda \sin(\beta) \\ -\sin(\beta)\sin(\delta) & \cos(\delta) & -\cos(\beta)\sin(\delta) & \lambda \cos(\beta)\sin(\delta) \\ \cos(\delta)\sin(\beta) & \sin(\delta) & \cos(\beta)\cos(\delta) & -\lambda \cos(\beta)\cos(\delta) \\ 0 & 0 & 0 & 1 \end{bmatrix}. \quad (A5)$$

The position vector  $\mathbf{R}_c^i$  can be obtained as:

$$\mathbf{R}_c^i = [\mathbf{M}_{cn}] \mathbf{R}_n^i, \quad (A6)$$

The components of the vector are:

$$\begin{aligned} x_c^i &= x_n^i \cos(\beta) + \lambda \sin(\beta), \\ y_c^i &= y_n^i \cos(\delta) + \lambda \cos(\beta) \sin(\delta) \\ &\quad - x_n^i \sin(\delta) \sin(\beta), \\ z_c^i &= y_n^i \sin(\delta) - \lambda \cos(\beta) \cos(\delta) \\ &\quad + x_n^i \cos(\delta) \sin(\beta). \end{aligned} \quad (A7)$$

Here,  $\lambda$  is the same offset parameter which is given in Eq. (6). In this way, coordinates of the 2D gear cross-sections can be calculated for an arbitrary value of tooth thickness in the axis of  $z$ . In the next step, the normal vectors of the cutting tool surfaces  $n_c^i$  should be calculated as:

$$n_c^i = \frac{\frac{\partial R_c^i}{\partial l_R} \times \frac{\partial R_c^i}{\partial \lambda_1}}{\left| \frac{\partial R_c^i}{\partial l_R} \times \frac{\partial R_c^i}{\partial \lambda_1} \right|}. \quad (A8)$$

Considering the rolling process, the relation between the rack cutter and the generated gear can be specified with the matrix  $\mathbf{M}_{1c}$ .

$$\mathbf{M}_{1c} = \begin{bmatrix} \cos(\varphi_1) & \sin(\varphi_1) & 0 & r_1(\sin(\varphi_1) - \varphi_1 \cos(\varphi_1)) \\ -\sin(\varphi_1) & \cos(\varphi_1) & 0 & r_1(\cos(\varphi_1) + \varphi_1 \sin(\varphi_1)) \\ 0 & 0 & 1 & 0 \\ 0 & 0 & 0 & 1 \end{bmatrix}. \quad (A9)$$

The roll angle of the generated gear  $\varphi_1$  can be calculated by considering the fundamental law of gearing.

$$\frac{X_c^i - x_c^i}{n_{xc}^i} = \frac{Y_c^i - y_c^i}{n_{yc}^i} = \frac{Z_c^i - z_c^i}{n_{zc}^i}, \quad (A10)$$

where  $X_c^i$ ,  $Y_c^i$  and  $Z_c^i$  are the coordinates of an arbitrary point on the instant center of rotation  $I-I$ . Detailed explanation is given in [6]. Here,  $n_{xc}^i$ ,  $n_{yc}^i$  and  $n_{zc}^i$  are the direction cosines of the unit normal

$n_c^i$ . Using this relation, the angle  $\phi_1$  can be obtained as:

$$\phi_1 = \frac{(y_c^i n_{xc}^i - x_c^i n_{yc}^i)}{r_p^i n_{xc}^i}. \quad (\text{A11})$$

After calculating the related parameters as specified, coordinates of the generated gear can be obtained by calculating the coordinate vector  $\mathbf{R}_1^i$ .

$$\mathbf{R}_1^i = [\mathbf{M}_{1c}] \mathbf{R}_c^i. \quad (\text{A12})$$

The calculation steps shows that, the position vector can not be obtained without calculating the roll angle  $\phi_1$ . Eq. (A11) requires the calculation of the unit normal  $n_c^i$ . The proposed mathematical method in this study, enables to complete the process without this calculation. The roll angle  $\phi$  can be calculated directly by Eq. (14) and the gear coordinates can be obtained by Eq. (12).